Involvement of TRPV4 in temperature-dependent perspiration in mice

Makiko Kashio[1,2 #], Sandra Derouiche[1 #], Reko U. Yoshimoto[3], Kenji Sano[4], Jing Lei[1,2], Mizuho A. Kido[3] and Makoto Tominaga[1,2,5 *]

[1] Division of Cell Signaling, National Institute for Physiological Sciences, National Institutes of Natural Sciences, 444-8787 Okazaki, Japan

[2] Thermal Biology Group, Exploratory Research Center on Life and Living Systems, National Institutes of Natural Sciences, 444-8787 Okazaki, Japan

[3] Division of Histology and Neuroanatomy, Department of Anatomy and Physiology, Faculty of Medicine, Saga University, 849-8501 Saga, Japan

[4] Department of Laboratory Medicine, Shinshu University Hospital, 390-8602 Matsumoto, Japan

[5] Department of Physiological Sciences, The Graduate University for Advanced Studies (SOKENDAI), 444-8585 Okazaki, Japan

# These authors contributed to this work equally.

*** Corresponding author**: Makoto Tominaga

Division of Cell Signaling, National Institute for Physiological Sciences, 5-1 Higashiyama, Myodaiji, Okazaki, Aichi, 444-8787, Japan

Tel: +81-564-59-5286, e-mail: tominaga@nips.ac.jp

ABSTRACT

Reports indicate that an interaction between TRPV4 and anoctamin 1 could be widely involved in water efflux of exocrine glands, suggesting that the interaction could play a role in perspiration. In secretory cells of sweat glands present in mouse foot pads, TRPV4 clearly colocalized with cytokeratin 8, anoctamin 1 (ANO1) and aquaporin-5 (AQP5). Mouse sweat glands showed TRPV4-dependent cytosolic Ca^{2+} increases that was inhibited by menthol. Acetylcholine-stimulated sweating in foot pads was temperature-dependent in wild-type, but not TRPV4-deficient mice, and was inhibited by menthol. Sweating could be important for maintaining friction forces in mouse foot pads, and this possibility is supported by the finding that wild-type mice climbed up a slippery slope more easily than TRPV4-deleted mice. Furthermore, TRPV4 expression was significantly higher in controls and normohidrotic skin from patients with AIGA (acquired idiopathic generalized anhidrosis) compared to anhidrotic skin from patients with AIGA. Collectively, TRPV4 is likely involved in temperature-dependent perspiration via interactions with anoctamin 1, and TRPV4 itself or the TRPV4 and anoctamin 1 complex would be targets to develop agents that regulate perspiration.

INTRODUCTION

Sweating is a vital physiological process.(Shibasaki & Crandall, 2010) There are two basic types of sweating: thermoregulatory and emotional sweating, in addition to gustatory sweating, largely localized to the face and neck regions, that occurs while consuming some foods, particularly pungent foods.(Lee, 1954) Most sweat glands are of the eccrine type, and they produce a thin secretion that is hypotonic to plasma. Although eccrine sweat glands are distributed all over the body, their density is highest in the axillary region and on the palms of the hands and the soles of the feet. In humans, the main function of eccrine sweat glands is body temperature regulation. Meanwhile, apocrine sweat glands are found primarily in the axillae and urogenital regions. These scent glands become active during puberty and secrete a viscous fluid that is associated with body odor.

Body temperature regulation is important to maintain a homeostasis. Body temperature is poorly controlled in patients with hypohidrosis. Meanwhile, patients affected by hyperhidrosis can have difficulty in social and professional situations due to increased sweat production, and the resulting subjective perception of illness at an individual level may be substantial.(Cohen & Solish, 2003; Schlereth et al., 2009) However, the molecular mechanisms of perspiration are not clearly understood.

We previously reported the functional interaction between TRP channels and the Ca^{2+}-activated Cl^- channel, anoctamin 1 (ANO1, also known as TMEM16A). (Derouiche et al., 2018;

Takayama et al., 2014, 2015) TRP channels have high Ca^{2+} permeability.(Gees et al., 2012) Ca^{2+} entering cells through TRP channels activates anoctamin 1 leading to Cl^- efflux that promotes formation of a physical complex in cells with high intracellular Cl^- concentrations. The Cl^- efflux may drive water efflux through water channels in exocrine gland acinar cells that increases exocrine function, and causes primary sensory neuron depolarization that increases nociception. For skin keratinocytes that have relatively low intracellular Cl^- concentrations, interaction between TRPV3 and ANO1 causes Cl^- influx, followed by increased cellular movement/proliferation in response to cell cycle modulation.(Yamanoi et al., 2023) Thus, direction of Cl^- movement through ANO1 is simply determined by the balance between equilibrium potentials of Cl^- and membrane potentials in each cell.(Takayama et al., 2019)

Involvement of TRPV4 in exocrine gland function prompted us to examine the functional interaction in perspiration, because TRPV4 is expressed in human eccrine sweat glands.(Delany et al., 2001) Although sweat glands are innervated by sympathetic neurons, acetylcholine is released from the nerve endings.(Hu et al., 2018) We show that the functional interaction of TRPV4 and ANO1 is involved in temperature-dependent sweating and increased friction force.

RESULTS

Expression of TRPV4, anoctamin 1 and AQP5 in mouse sweat glands

We detected expression of TRPV4, ANO1 and the water channel aquaporin-5 (AQP5) in eccrine glands of mouse foot pads. The secretory coil is located in the deep dermis and a relatively straight duct opens to the skin surface. We first validated an anti-TRPV4 antibody that we generated. This anti-TRPV4 antibody conspicuously labeled the basal layer of the epidermis, secretory eccrine gland cells, and duct cells only in skin from wild-type (WT) mice, but not in skin from TRPV4-deficient (TRPV4KO) mice (Figure 1A), indicating the antibody specificity. TRPV4 was clearly localized in secretory glands as confirmed by positivity for cytokeratin 8 (CK8), a secretory cell marker (Figure 1B). The duct cells were not labeled by ANO1 and CK8 (Figure 1B). TRPV4-immunoreactivity was stronger in duct cells near the secretory region and gradually diminished in the distal excretory ducts toward the epidermis. Bilayered sweat ducts showed TRPV4 labeling in basal cells but not suprabasal cells (Figure 1C). Secretory cells in human eccrine glands are classified into two types: clear cells that mainly secrete water and electrolytes, and dark cells that secrete macromolecules like glycoproteins. We found that TRPV4-expressing secretory cells were positive for the calcitonin gene-related peptide (CGRP), a dark cell marker, and were heterogeneously labeled (Figure 1D). This result is consistent with earlier studies showing that mouse eccrine glands have a more primitive structure than human glands, and have only one type of secretory cell that

resembles human clear cells but also has dark cell characteristics.(Bovell, 2018; Kurosumi & Kurosumi, 1970)

To explore TRPV4 subcellular localization, we observed tissues using Airyscan super-resolution imaging. TRPV4 was heterogeneously labeled in the gland cells, and showed apparent localization in basal and apical membranes (Figure 1D). TRPV4 was absent in myoepithelial cells. Conspicuous co-labeling of TRPV4 and ANO1 or AQP5 with filamentous actin (F-actin) was seen at the apical site (luminal side) of the secretory cells (Figure 1E). These close topological relationships clearly suggest that TRPV4, ANO1 and AQP5 would be able to form a complex that promotes sweat secretion in eccrine glands of mouse foot pads. These results also suggest that TRPV4-expressing secretory cells are involved in secretion of macromolecular components as well as secretion of water and ions.

Functional expression of TRPV4 in acinar cells of mouse sweat glands

Next, we examined functional TRPV4 expression. WT mouse sweat glands responded to the TRPV4 agonist, GSK (500 nM) and to acetylcholine (Ach, 10 μM) (Figure 2A). No cytosolic Ca^{2+} increase induced by GSK was observed in sweat glands from TRPV4KO mice (Figure 2B). Interestingly, the GSK-induced increase in cytosolic Ca^{2+} was significantly inhibited by menthol (5 μM) in WT mouse sweat glands, suggesting that menthol inhibited TRPV4 function. Meanwhile, menthol alone caused no change in cytosolic Ca^{2+} concentration (Figure 2C). These data indicated functional expression of TRPV4 in secretory cells.

TRPV4 involvement in perspiration in mice

To examine the functional interaction between TRPV4 and ANO1 in mouse sweat glands *in vivo*, stimulated sweating induced by Ach (100 μM, 2 min) in mouse hind paws at 25 ˚C and 35 ˚C was investigated using an iodine and starch reaction to measure secreted amylase.(Nejsum et al., 2002) At 25 ˚C, no difference in stimulated sweating was seen between WT and TRPV4KO. However, at 35 ˚C, stimulated sweating tended to increase in WT mice with no similar increase seen for TRPV4KO, although the difference between WT and TRPV4KO mice did not statistically differ (Figure 3A, B). Temperature-dependent basal sweating without stimulation for 15 min was also observed for WT mice, but not in TRPV4KO mice and this difference was statistically significant (Figure 3C, D). Menthol inhibits both TRPV4 (Figure 2C) and ANO1 function.(Takayama et al., 2017) The ability of menthol to inhibit both TRPV4 and ANO1 suggests that menthol would inhibit sweating. Accordingly, we compared stimulated sweating with either ethanol vehicle (used for menthol dilution) or menthol treatment for 2 min. Menthol treatment caused a significantly lower degree of

sweating than ethanol treatment (Figure 3E, F). This result could indicate that menthol inhibits sweating by inhibiting the function of both TRPV4 and ANO1.

Physiological significance of TRPV4-mediated sweating

Mice do not sweat to control body temperature, so the physiological significance of hind paw sweating is unclear. In humans, fingertip moisture is known to be optimally modulated during object manipulation through regulation of friction force.(André et al., 2010) The same mechanism might promote for traction of hind paws when mice climb slippery slopes. Here we constructed a slope covered with slippery vinyl (Figure 4A) and compared climbing behaviors of WT and TRPV4KO for 1 hour at 26-27 ˚C with 35-50% humidity. The total number of climbing attempts was the same for WT and TRPV4KO mice (25.6 ± 2.5 for WT, n = 5; 24.7 ± 3.9 for TRPV4KO, n = 4) (Figure 4B), but a higher percentage of WT mice successfully climbed to the top of the slope than did TRPV4KO mice (79.5 ± 6.4% for WT; 41.8 ± 2.8% for TRPV4KO; $p < 0.01$) (Figure 4CD) (Suppl. video). And WT mice easily came down the slippery slope. These data suggest that WT mice might produce more hind paw sweat (Figure 3) that increases traction on the slope.

TRPV4 expression in human sweat glands

We next examined whether TRPV4 also plays a role in human perspiration. Patients with acquired idiopathic generalized anhidrosis (AIGA) have acquired impairment in total body sweating even when exposed to heat or engaging in exercise.(Munetsugu et al., 2017; Nakazato et al., 2004; Sano et al., 2017) We compared TRPV4 expression in sweat glands from patients with melanocytic nevus (n = 10, ages; 15 – 63) as controls and patients with AIGA (n = 10, ages; 24 - 55). All patients with AIGA were male, which is consistent with the gender distribution of AIGA, while two of the 10 controls were female. Representative TRPV4 staining is shown in Figure 5A, B. Although signals for TRPV4 staining were high in normohidrotic skin from a patient with AIGA and were equivalent to those of controls, levels in anhidrotic skin from the same patient with AIGA were very low.

We classified TRPV4 staining intensity from 1+ (low) to 3+ (high). Scores were significantly higher in controls and normohidrotic skin from patients with AIGA (2+ or 3+) than anhidrotic skin from AIGA cases (1+ or 2+) (mean 2.5 ± 0.17 vs 1.0 ± 0.10 for controls and normohidrotic skin from patients with AIGA vs. anhidrotic skin from AIGA cases, respectively, $p < 0.0001$) (Figure 5). These data clearly indicated that TRPV4 plays a role in normal perspiration in humans.

DISCUSSION

Ca^{2+} entering cells through TRP channels is known to be involved in various Ca^{2+}-mediated events, particularly in non-excitable cells, whereas cation influx-induced depolarization is important for excitation of primary sensory neurons through activation of voltage-gated Na^{+} channels.(Derouiche et al., 2018; Takayama et al., 2014, 2015) Ca^{2+} entering cells is instantaneously chelated to maintain low intracellular Ca^{2+} concentrations. However, high Ca^{2+} conditions can persist for longer periods just beneath the plasma membrane. We reported that several TRP channels including TRPV1, TRPV3, TRPV4 and TRPA1 can form a complex with the Ca^{2+}-activated Cl^{-} channel, ANO1, and activate ANO1 via Ca^{2+} entering cells through TRP channels.[5–7] Interaction between TRPV4 and ANO1 causes Cl^{-} efflux, followed by water efflux, suggesting that the complex could be involved in exocrine gland functions including secretion of cerebrospinal fluid, saliva and tears.(Derouiche et al., 2018; Takayama et al., 2014) We demonstrated that the TRPV4-ANO1 interaction is also involved in water efflux associated with the exocrine function during sweating in this study. Digestive secretion could also involve this interaction. Notably, the TRPV4, ANO1 and AQP5 complex is confined to acinar cells in secretory sweat glands, whereas TRPV4 is also expressed at other sites in skin tissues (Figure 1). This result could indicate a specific function for the complex in water efflux occurring in exocrine glands.

Several human diseases involve hypohidrosis or hyperhidrosis.(Cheshire, 2020; Cohen & Solish, 2003; Schlereth et al., 2009) Patients with hypohidrosis have difficulty regulating body temperature in response to high temperatures and can experience dizziness, muscle cramps, weakness, high fever or nausea that is typically not serious. However, patients with hypohidrosis sometimes have heatstroke, which is the most serious complication; the incidence of heatstroke has recently increased with global warming. Furthermore, some patients with collagen diseases like Sjögren's syndrome, an autoimmune exocrinopathy, suffer from hypohidrosis as well as dry mouth and dry eye that is not easily treated.(Katayama, 2018) AIGA is also characterized by hypohidrosis without clear etiology.(Munetsugu et al., 2017; Nakazato et al., 2004; Sano et al., 2017) In Japan, both Sjögren's syndrome and AIGA are classified as designated intractable diseases (No. 53 and 163, respectively). Problems with exocrine gland function in Sjögren's syndrome patients as well as the low TRPV4 expression levels in patients with AIGA suggest that TRPV4 could be a key molecule involved in these diseases and that novel treatment strategies could target TRPV4 and/or ANO1.

The application of menthol to the skin produces a cool sensation that is generally thought to result from the activation of the menthol receptor TRPM8. However, the finding here that menthol inhibits both TRPV4 and ANO1 suggests that transient reduction in sweating by inhibiting formation of the TRPV4-ANO1 complex also contributes to the cool sensation. On the other hand, patients with hyperhidrosis can sweat enough to soak their clothing or have

sweat drip off their hands (Cohen & Solish, 2003; Schlereth et al., 2009). Hyperhidrosis can occur as a primary or secondary effect after infections or with some endocrine diseases. Others can experience hyperhidrosis on the palms of their hands when nervous. Development of chemicals targeting TRPV4, ANO1 or the complex could be a new therapeutic strategy for these conditions, for which there are currently no effective treatments.

Many TRP channels have high Ca^{2+} permeability, suggesting that Ca^{2+} entering cells through TRP channels in turn activates more Ca^{2+}-activated proteins including other Ca^{2+}-activated ion channels such as Ca^{2+}-activated K^+ channels. This interaction could expand the importance of TRP channels in physiological functions, and complexes between TRP channels and Ca^{2+}-activated proteins would be novel targets for drug development.

MATERIALS AND METHODS

Mice

Homozygous TRPV4-deficient (TRPV4KO) mice from Makoto Suzuki (Jichi Medical University) (Mizuno et al., 2003) were maintained under SPF conditions in a controlled environment (12-hour light/dark cycle with free access to food and water, 25 °C, and 50-60% humidity). All procedures were approved by the Institutional Animal Care and Use Committee of the National Institute of Natural Sciences (Approval No. 21A008) and carried out according to the National Institutes of Health and National Institute for Physiological Sciences guidelines.

Human ethics

Informed consent was obtained from all patients, and the study was approved by the Shinshu University Ethics Committee (Approval No. 4073). Anhidrotic or hypohidrotic as well as normohidrotic skin samples taken from various sites were collected from 10 patients who were clinically diagnosed with acquired idiopathic generalized anhidrosis (AIGA) using standard criteria set by the Japan AIGA study group (Revised guideline for the diagnosis and treatment of acquired idiopathic generalized anhidrosis in Japan) (Munetsugu et al., 2017).

Chemicals

Collagenase A, trypsin from soybean, ionomycin calcium salt, acetylcholine, carbachol, and GSK1016790A (G0798) were purchased from Sigma (St. Louis, MO, USA). T16Ainh-A01 was purchased from Calbiochem (San Diego, CA, USA, 613551).

Isolation of sweat glands from mice

Dissected tips of digits and foot pads of mice were minced and incubated in 0.25mg/mL liberase TL (Roche, 5401119001) for 45 min at 37 ˚C with pipetting every 10min. The digested tissue suspension was filtered through a 40mm cell strainer, and the isolated sweat glands

were retained in the filter. The collected sweat glands were seeded on Cell-Tak-coated glass slips and used for Ca2+-imaging analysis after incubation at 37 ˚C (>2h) in DMEM supplemented with 10% fetal bovine serum, penicillin-streptomycin and Glutamax.

Mouse immunostaining

Experiments were performed using 8- to 21-wk-old male and female mice. Mice (n = 4 per group) were anesthetized with a combination of hydrochloric acid medetomidine (0.75mg/kg; Kyoritsu Seiyaku, Tokyo, Japan), butorphanol (5mg/kg; Meiji Seika Pharma, Tokyo, Japan), and midazolam (4mg/kg, Maruishi, 21-3981), and perfused transcardially with heparinized PBS followed by 4% paraformaldehyde in phosphate buffer (pH 7.4). The hind paw pad skin was dissected and post-fixed in 4% PFA for 3 h at 4 ˚C, cryoprotected with 20% sucrose overnight and then embedded in OCT compound. For immunohistochemistry, 5μm-thick frozen sections were made with a NX50 cryostat. Sections were permeabilized with 0.3% Triton-X100 in PBS for 10 min at room temperature and then incubated with a blocking solution, PBS supplemented with 0.3% Triton X-100, 1% bovine serum albumin, 0.05% sodium azide and 5% normal donkey serum for 45 min at room temperature. Sections were then incubated overnight at 4 °C with the primary antibodies: guinea pig anti-TRPV4 (2 μg/mL) (Kitsuki et al., 2020), rabbit anti-ANO1 (1:100, Abcam, ab53213), rabbit anti-AQP5 (1:200, Millipore, 178615), rabbit anti-CGRP (1:2000, Amersham International, RPN.1842), rat anti-cytokeratin 8 (CK8) (1:100, Millipore, MABT329), and rat anti-E-cadherin (1:200, Takara Bio, M108). Next, sections were incubated for 1h at room temperature with the secondary antibodies: Alexa Fluor 488 donkey anti-guinea pig IgG, Alexa Fluor 555 donkey anti-rabbit IgG, Alexa Fluor 647 donkey anti-rat IgG (all 1:200, Jackson ImmunoResearch Labs). F-actin was visualized with Phalloidin-iFluor 647 Reagent (1:1000). After immunostaining, sections were incubated for 5 min with 4',6-diamidino-2-phenylindole, dihydrochloride (DAPI, Dojindo, D523) and then mounted with PermaFluor (Thermo Fisher Scientific). Images were acquired using a BC43 or LSM800 instrument equipped with a Zeiss Axio Observer Z1 and a LSM 800 confocal unit with Airyscan module. For super-resolution imaging, images of optical 160 nm-thick slices were taken with a Plan Apochromat 63×/1.40 NA Oil DIC M27 objective. Images were processed with Airyscan processing in ZEN blue 3.5 software.

Human immunostaining

Immunohistochemical analysis of formalin-fixed paraffin embedded tissue sections (2-3 μm-thick) of anhidrotic and normohidrotic skin samples from 10 patients with AIGA. Except for application of primary antibody (100x) all steps including deparaffinization, blocking of internal peroxidase activity, unmasking of specific antigen, application of secondary antibody,

detection of signals and nuclear staining were automatically performed by a Ventana auto-staining system. Skin samples with melanocytic nevus (n=10) were used as a control.

Calcium imaging

After loading with Fura-2 AM (5 μM, Invitrogen, F-1201), isolated sweat glands on coverslips were mounted in an open chamber and rinsed with standard bath solution containing (in mM): 140 NaCl, 5 KCl, 2 $MgCl_2$, 2 $CaCl_2$, 10 HEPES, and 10 glucose, pH 7.4. The intracellular free calcium concentration in isolated sweat glands was measured by dual-wavelength fura-2 microfluorometry with excitation at 340/380 nm and emission at 510 nm. The ratio image was calculated and acquired using the IP-Lab imaging processing system.

Mouse climbing experiments

WT and TRPV4KO mice were allowed to acclimate for one day prior to recording in a cage containing a slippery slope made with vinyl. Mice were housed for 1 hour in the cage with the slope at 26-27 ˚C and 35-50% humidity. Climbing and slipping behaviors were videotaped and analyzed.

Quantifications and statistical analysis

Data are shown as mean ± sem. Statistical analysis was performed with Origin Pro 8. Student's t-test and two-way ANOVA with Dunnett's or Bonferroni's multiple-comparison tests were performed for comparisons. Values of $p < 0.05$ indicate statistical significance.

ACKNOWLEDGEMENTS

This work was supported by grants to MT from a Grant-in-Aid for Scientific Research from the Ministry of Education, Culture, Sports, Science and Technology in Japan (#20H05768, #21H02667 and #23H04943).

AUTHOR CONTRIBUTION

M.K., S.D, R.U.Y., K.S., J.L. and M.A.K. designed and performed the experiments. M.A.K. and M.T. wrote the paper.

REFERENCES

André, T., Lefèvre, P., & Thonnard, J.-L. (2010). Fingertip Moisture Is Optimally Modulated During Object Manipulation. *Journal of Neurophysiology*, *103*(1), 402–408. https://doi.org/10.1152/jn.00901.2009

Bovell, D. L. (2018). The evolution of eccrine sweat gland research towards developing a model for human sweat gland function. *Experimental Dermatology*, *27*(5), 544–550. https://doi.org/10.1111/exd.13556

Cheshire, W. P. (2020). Sudomotor Dysfunction. *Seminars in Neurology*, *40*(05), 560–568. https://doi.org/10.1055/s-0040-1713847

Cohen, J. L., & Solish, N. (2003). Treatment of hyperhidrosis with botulinum toxin. *Facial Plastic Surgery Clinics of North America*, *11*(4), 493–502. https://doi.org/10.1016/S1064-7406(03)00091-9

Delany, N. S., Hurle, M., Facer, P., Alnadaf, T., Plumpton, C., Kinghorn, I., See, C. G., Costigan, M., Anand, P., Woolf, C. J., Crowther, D., Sanseau, P., & Tate, S. N. (2001). Identification and characterization of a novel human vanilloid receptor-like protein, VRL-2. *Physiological Genomics*, *4*(3), 165–174. https://doi.org/10.1152/physiolgenomics.2001.4.3.165

Derouiche, S., Takayama, Y., Murakami, M., & Tominaga, M. (2018). TRPV4 heats up ANO1-dependent exocrine gland fluid secretion. *The FASEB Journal*, *32*(4), 1841–1854. https://doi.org/10.1096/fj.201700954R

Gees, M., Owsianik, G., Nilius, B., & Voets, T. (2012). TRP Channels. In *Comprehensive Physiology* (pp. 563–608). John Wiley & Sons, Ltd. https://doi.org/10.1002/cphy.c110026

Hu, Y., Converse, C., Lyons, M. C., & Hsu, W. H. (2018). Neural control of sweat secretion: A review. *British Journal of Dermatology*, *178*(6), 1246–1256. https://doi.org/10.1111/bjd.15808

Katayama, I. (2018). Dry skin manifestations in Sjögren syndrome and atopic dermatitis related to aberrant sudomotor function in inflammatory allergic skin diseases. *Allergology International*, *67*(4), 448–454. https://doi.org/10.1016/j.alit.2018.07.001

Kitsuki, T., Yoshimoto, R. U., Aijima, R., Hatakeyama, J., Cao, A., Zhang, J., Ohsaki, Y., Mori, Y., & Kido, M. A. (2020). Enhanced junctional epithelial permeability in TRPV4-deficient mice. *Journal of Periodontal Research*, *55*(1), 51–60. https://doi.org/10.1111/jre.12685

Kurosumi, K., & Kurosumi, U. (1970). Electron Microscopy of the Mouse Plantar Eccrine Sweat Glands. *Archivum Histologicum Japonicum*, *31*(3–4), 455–475. https://doi.org/10.1679/aohc1950.31.455

Lee, T. S. (1954). Physiological gustatory sweating in a warm climate. *The Journal of Physiology*, *124*(3), 528–542. https://doi.org/10.1113/jphysiol.1954.sp005126

Mizuno, A., Matsumoto, N., Imai, M., & Suzuki, M. (2003). Impaired osmotic sensation in mice lacking TRPV4. *American Journal of Physiology-Cell Physiology*, *285*(1), C96–C101. https://doi.org/10.1152/ajpcell.00559.2002

Munetsugu, T., Fujimoto, T., Sano, K., Murota, H., Satoh, T., Iwase, S., Asahina, M., Nakazato, Y., & Yokozeki, H. (2017). Revised guideline for the diagnosis and treatment of acquired idiopathic generalized anhidrosis in Japan. *The Journal of Dermatology*, *44*(4), 394–400. https://doi.org/10.1111/1346-8138.13649

Nakazato, Y., Tamura, N., Ohkuma, A., Yoshimaru, K., & Shimazu, K. (2004). Idiopathic pure sudomotor failure: Anhidrosis due to deficits in cholinergic transmission. *Neurology*, *63*(8), 1476–1480. https://doi.org/10.1212/01.WNL.0000142036.54112.57

Nejsum, L. N., Kwon, T.-H., Jensen, U. B., Fumagalli, O., Frøkiaer, J., Krane, C. M., Menon, A. G., King, L. S., Agre, P. C., & Nielsen, S. (2002). Functional requirement of aquaporin-5 in plasma membranes of sweat glands. *Proceedings of the National Academy of Sciences of the United States of America*, *99*(1), 511–516. https://doi.org/10.1073/pnas.012588099

Sano, K., Asahina, M., Uehara, T., Matsumoto, K., Araki, N., & Okuyama, R. (2017). Degranulation and shrinkage of dark cells in eccrine glands and elevated serum carcinoembryonic antigen in patients with acquired idiopathic generalized anhidrosis. *Journal of the European Academy of Dermatology and Venereology*, *31*(12), 2097–2103. https://doi.org/10.1111/jdv.14443

Schlereth, T., Dieterich, M., & Birklein, F. (2009). Hyperhidrosis—Causes and Treatment of Enhanced Sweating. *Deutsches Ärzteblatt International*, *106*(3), 32–37. https://doi.org/10.3238/arztebl.2009.0032

Shibasaki, M., & Crandall, C. G. (2010). Mechanisms and controllers of eccrine sweating in humans. *Frontiers in Bioscience (Scholar Edition)*, *2*, 685–696.

Takayama, Y., Derouiche, S., Maruyama, K., & Tominaga, M. (2019). Emerging Perspectives on Pain Management by Modulation of TRP Channels and ANO1. *International Journal of Molecular Sciences*, *20*(14), 3411. https://doi.org/10.3390/ijms20143411

Takayama, Y., Furue, H., & Tominaga, M. (2017). 4-isopropylcyclohexanol has potential analgesic effects through the inhibition of anoctamin 1, TRPV1 and TRPA1 channel activities. *Scientific Reports*, *7*(1), Article 1. https://doi.org/10.1038/srep43132

Takayama, Y., Shibasaki, K., Suzuki, Y., Yamanaka, A., & Tominaga, M. (2014). Modulation of water efflux through functional interaction between TRPV4 and TMEM16A/anoctamin 1. *The FASEB Journal*, *28*(5), 2238–2248. https://doi.org/10.1096/fj.13-243436

Takayama, Y., Uta, D., Furue, H., & Tominaga, M. (2015). Pain-enhancing mechanism through interaction between TRPV1 and anoctamin 1 in sensory neurons. *Proceedings of the National Academy of Sciences*, *112*(16), 5213–5218. https://doi.org/10.1073/pnas.1421507112

Yamanoi, Y., Lei, J., Takayama, Y., Hosogi, S., Marunaka, Y., & Tominaga, M. (2023). TRPV3-ANO1 interaction positively regulates wound healing in keratinocytes. *Communications Biology*, *6*(1), Article 1. https://doi.org/10.1038/s42003-023-04482-1

FIGURES

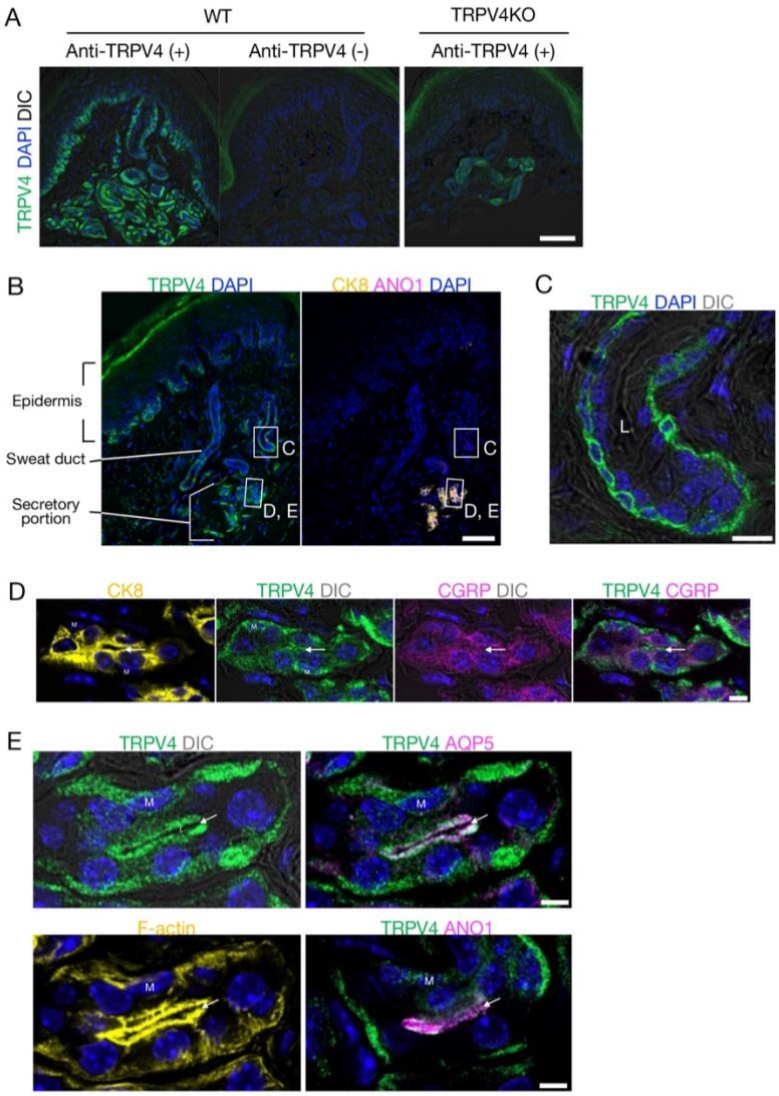

Figure 1. TRPV4 localization in eccrine glands of mouse foot pads.

(A) TRPV4 signals in the secretory coil in the deep dermis with a relatively straight duct opening to the skin surface. (B) Localization of TRPV4 (green), cytokeratin 8 (CK8; yellow) and anoctamin 1 (ANO1; magenta) in the skin. (C, D, E) Highly magnified Airyscan super-resolution images of the sweat duct (C) and secretory portion (D, E). (C) TRPV4 localizes to the basal cells of the bilayered sweat duct. Ductal lumen: L. (D) Secretory gland showing labeling for TRPV4 and calcitonin gene-related peptide (CGRP). (E) Secretory gland with conspicuous TRPV4 labeling in myoepithelial cells (M) and secretory cells. TRPV4 clearly colocalizes with aquaporin-5 (AQP5), F-actin, and ANO1 at the luminal side of the secretory cells. Arrows indicate the glandular lumen. Differential interference contrast: DIC, Nuclei: DAPI. Scale bar: 50 μm (A, B). 5 μm (C-E).

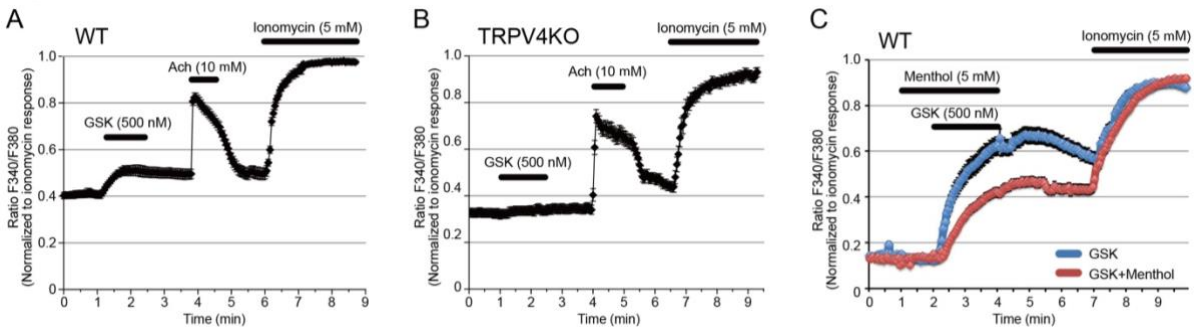

Figure 2. Functional TRPV4 expression in mouse sweat gland acinar cells.

(A, B) Changes in cytosolic Ca^{2+} concentrations upon stimulation with GSK, acetylcholine or ionomycin in sweat gland acinar cells from wild-type (WT, A) and TRPV4-deficient (TRPV4, B) mice. n=6 for Wt and TRPV4KO sweat glands. (C) Changes in cytosolic Ca^{2+} concentration upon stimulation with GSK in the presence (red) or absence (blue) of menthol in sweat gland acinar cells from WT mice.

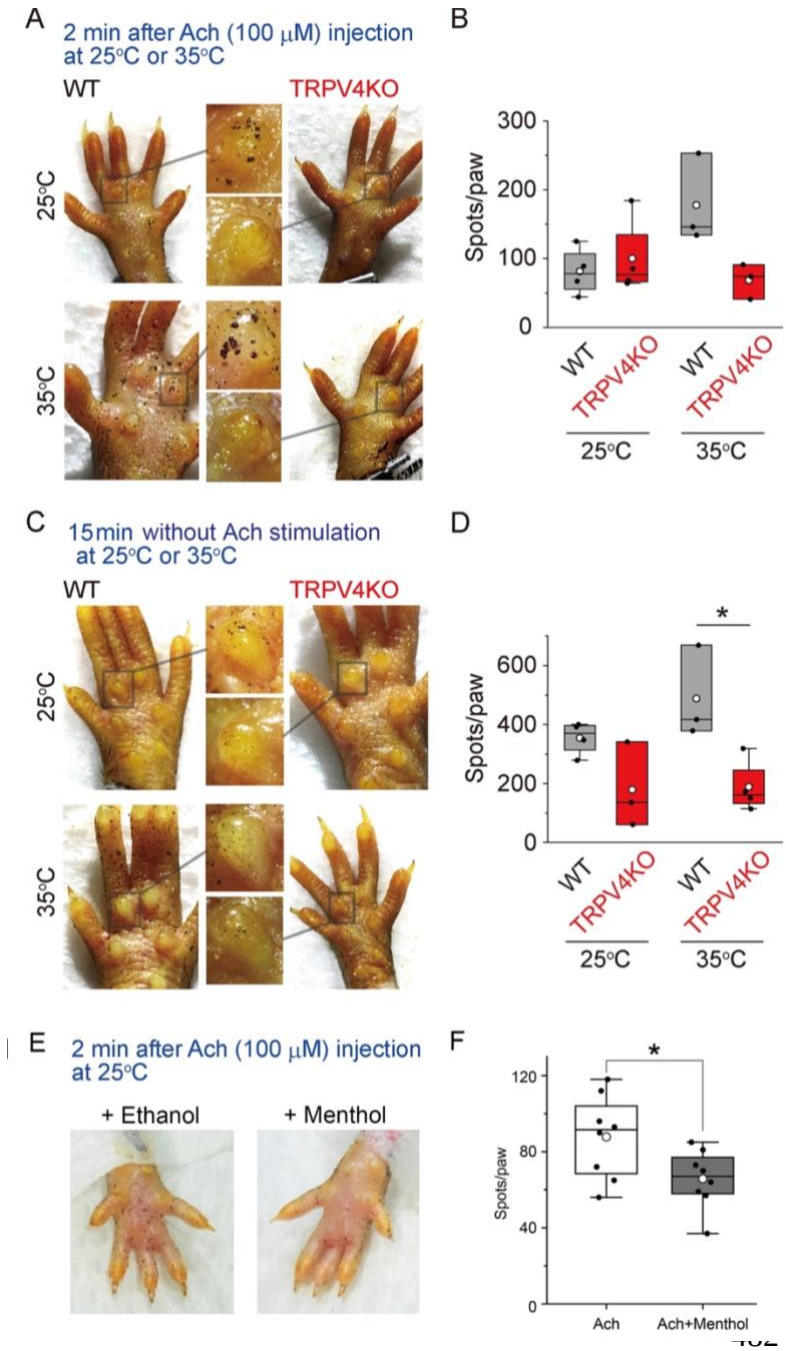

Figure 3. Stimulated sweating in mouse hind paws at different temperatures. (A) Representative stimulated sweat spots formed at 25 ˚C or 35 ˚C in hind paws of WT and TRPV4KO mice 2 min after injection of acetylcholine. (B) Comparison of sweat spots/paws at 25 ˚C or 35 ˚C in WT and TRPV4KO mice (box-whisker plot). n = 3~4 for WT or TRPV4KO. (C) Representative stimulated sweat spots at 25 ˚C or 35 ˚C in hind paws of WT and TRPV4KO mice without acetylcholine stimulation at 15 min. (D) Comparison of sweat spots/paw at 25 ˚C or 35 ˚C for WT and TRPV4KO mice (box-whisker plot). n = 3~4 for WT or TRPV4KO. (E) Representative stimulated sweat spots at 25 ˚C in hind paws of WT mice 2 min after injection of acetylcholine with or without menthol. (F) Comparison of sweat spots/paw at 25 ˚C in WT mice (box-whisker plot). n = 8 for with or without menthol. * $p < 0.05$.

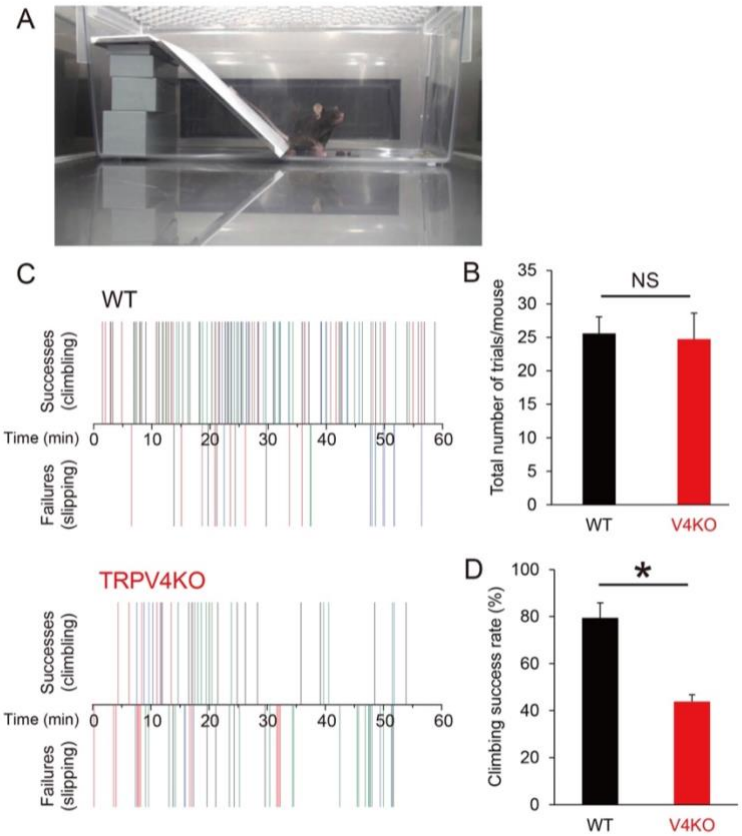

Figure 4. Climbing behaviors on a slippery slope.

(A) A mouse in a cage containing the vinyl slope. (B) Number of attempts made by WT and TRPV4KO mice within 60 min. (C) Successful (climbing) and failed (slipping) climbing behaviors exhibited by WT and TRPV4KO mice within 60 min. Different colors indicate individual mice. n = 5 for both WT and TRPV4KO. (D) Comparison of climbing success rates between WT and TRPV4KO mice. * $p < 0.05$.

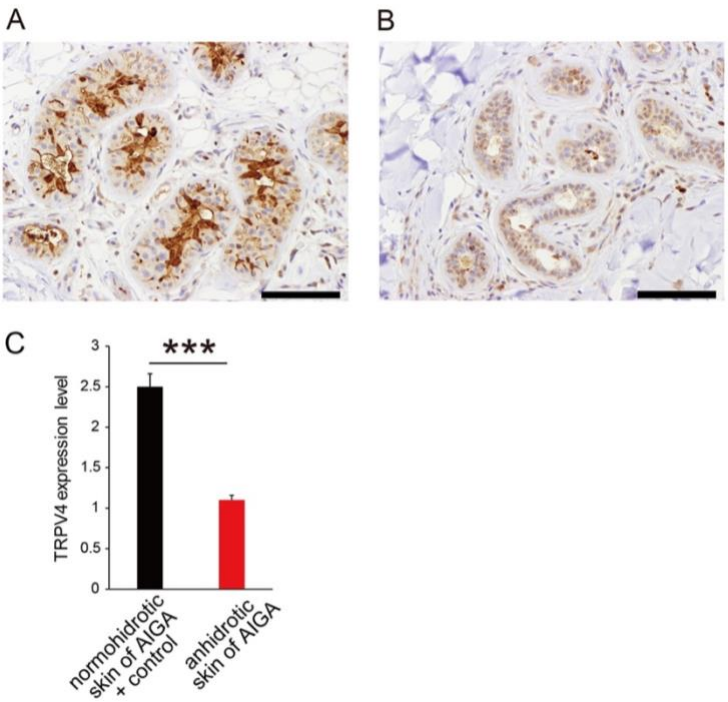

Figure 5. TRPV4 expression in human sweat glands.

Representative TRPV4 staining in sweat glands from normohidrotic (A) and anhidrotic (B) skin from the same patient with AIGA. Scales bars: 50 μm. (C) Scored TRPV4 expression levels in normohidrotic skin from patients with AIGA and Controls (melanocytic nevus) versus anhidrotic skin from patients with AIGA. *** $p < 0.001$.

supplementary video legends

1. **SI video 1 (WT)**
   WT mice successfully climbed to the top of the slippery slope, and easily came down the slope.

2. **SI video 2 (TRPV4KO)**
   TRPV4KO mice failed to climb to the top of the slippery slope.